Available online at www.sciencedirect.com

ScienceDirect

Journal of Electrocardiology 47 (2014) 826 – 830

JOURNAL OF Electrocardiology

www.jecgonline.com

# Extraction of respiratory myogram interference from the ECG and its application to characterize sleep-related breathing disorders in atrial fibrillation

Christoph Maier, PhD, [a, b,*] Hartmut Dickhaus, PhD [a]

[a] *Heidelberg University, Institute of Medical Biometry and Informatics, Heidelberg, Germany*
[b] *Heilbronn University, Faculty of Informatics, Heilbronn, Germany*

**Abstract**

**Background and purpose:** Present methods to extract respiratory myogram interference (RMI) from the Holter-ECG and assess effect of supraventricular arrhythmias (SVAs) onto ECG-based detection of sleep-related breathing disorders (SRBDs) and AHI estimation.
**Methods:** RMI was quantified as residual energy after ECG cancellation or high-pass filtering for different windowing constellations. In 140 cases without (SET_A) and 10 cases with persistent SVAs (SET_B), respiratory polysomnogram annotations served as reference for SRDB detection from Holter-ECGs. We applied our previously published method to identify SRDBs in 1-min epochs and estimate the AHI based on joint modulations in RMI and QRS-area.
**Results:** Sensitivity and specificity of 0.855/0.860 in SET_A dropped to 0.831/0.75 in SET_B. A significantly higher number of wake events in SET_B likely contribute to the asymmetric decrease and is consistent with a tendency to overestimate the AHI.
**Conclusions:** Despite reduced accuracy, RMI and QRS-area appear relatively robust against SVA and promise Holter-based detection at least of medium to severe SRBDs also in patients with SVAs.


*Keywords:* Sleep-related breathing disorders; ECG-derived respiration; Supraventricular arrhythmia; Atrial fibrillation; Sleep apnea; ECG; Respiratory myogram interference; QRS amplitude

## Introduction

The biomedical signal processing problem of extracting respiratory information from the ECG has attracted the interest of researchers over a history of at least 40 years [1]. Paired with a demand for simpler, cheaper and robust diagnostic means facilitating earlier recognition, the increasing awareness of the adverse cardiovascular consequences of sleep-related breathing disorders (SRDBs).

[2] has recently re-triggered this interest [3]. In this context, many groups focus on heart rate reflexes [4] or respiratory modulation of the QRS amplitude [5]. Remarkably, one source of information already mentioned by Einthoven [6] has rarely been exploited: the respiratory myogram interference (RMI) in the ECG.

Combined with a measure of QRS amplitude, we have successfully applied RMI to identification of SRDBs in substantial collectives comprising patients largely free from arrhythmias [7]. Principally, we expect both quantities, QRS amplitude and RMI, to be largely robust against arrhythmias at least of supraventricular origin. To check the applicability in this clinically important condition which is not uncommon for SRBDs, we apply our previously developed technique to a small set of patients with supraventricular arrhythmias (SVAs) and compare the results to the arrhythmia-free case. Moreover, we cover some methodological aspects of RMI extraction.

## Methods

### *Data*

Over a period of 18 months, simultaneous registrations of Holter-ECGs (Mortara H12+, 8 channels, 1 kHz/ch.) and polysomnograms (PSGs, Alice 4) were taken in 150 cases suspected for sleep-related breathing disorders in the Sleep Medicine Center of the Thoraxklinik Heidelberg. In 140 cases (121 patients, 16 females), the ECG contained less than 5 % ectopy (8% in one case). We refer to these data as set A

* Corresponding author at: Heidelberg University, Department of Medical Biometry and Informatics, Im Neuenheimer Feld 305, 69120 Heidelberg, Germany.
*E-mail address:* christoph.maier@med.uni-heidelberg.de

http://dx.doi.org/10.1016/j.jelectrocard.2014.07.017
0022-0736/

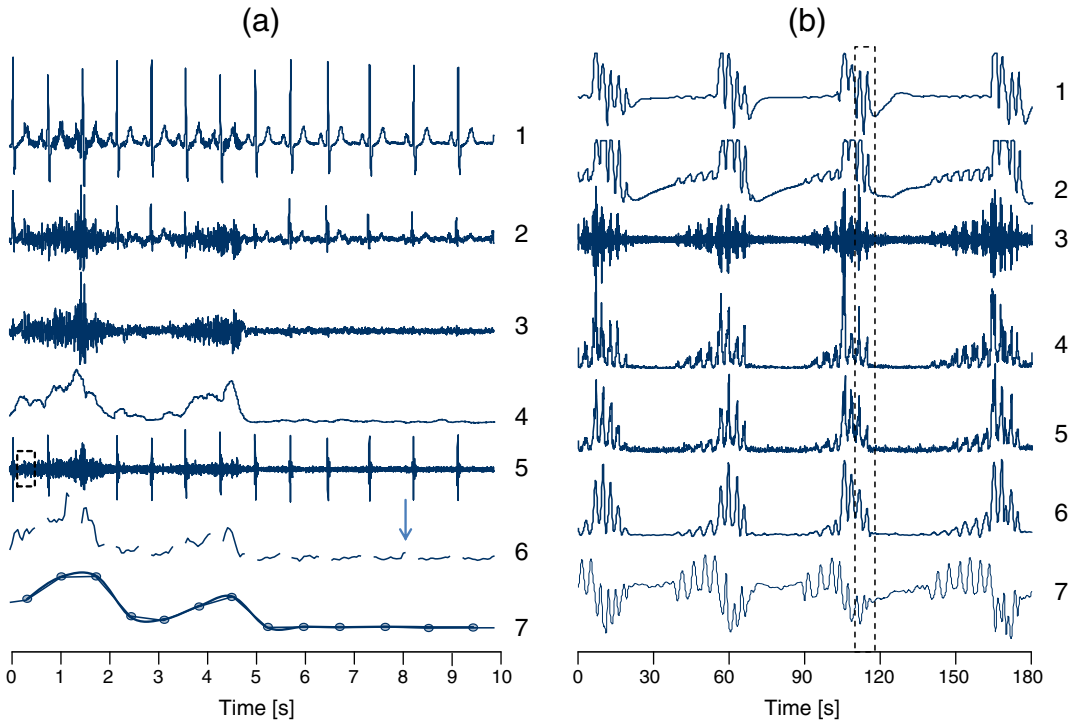


Fig. 1. (a) RMI extraction and quantification (1). ECG with RMI (2). Residuals after template subtraction (3). Residuals (i.e. RMI) after complete ECG elimination (4). Quantification of RMI as SD of trace 3 in sliding 100 ms window (5). ECG shown in trace 1 after 60 Hz high-pass filter (6). Quantification of RMI as SD of trace 5 in sliding 100 ms window. The QRS region (R ± 50 ms) is excluded producing the gaps in the trace (7). Quantification of RMI as beat-to-beat series (M*-series). The ordinate of each dot represents the SD of trace 5 calculated in a window covering the T-wave region [R + 80 ms;R + 430 ms] of the corresponding cycle. The first window is shown as dashed rectangle in trace 5. The lines represent the linear and cubic spline interpolation of the dots (M-series). (b) Exemplary time-courses of measured (traces 1–2) and ECG-derived (traces 3–7) respiratory signals during repetitive mixed apneas. The dashed rectangle corresponds to the time axis of the left-hand graph (a). Traces 4-7 were re-sampled ad 10 Hz (1). Respiratory flow and (2) abdominal effort from the PSG (3). RMI after ECG cancellation (4). Quantification of RMI as SD of trace 3 in sliding 100 ms window (5). Quantification of RMI as SD of the 60 Hz high-pass filtered ECG in sliding 100 ms window with QRS region excluded (6). Quantification of RMI as SD of the 60Hz high-pass filtered ECG in a window covering the T-wave region (M-series) (7). Q-series of absolute areas under the QRS complex.

and have reported results for this set earlier [7]. Set B consists of 10 cases (1 female) with persistent supraventricular arrhythmias, and serves as a test to which extent the results obtained earlier on set A are reproducible under arrhythmic conditions. In 9/10 set-B-subjects atrial fibrillation persists for the entire duration of the recording. The other case suffers from a focal atrial ectopy that interferes with the sinus-rhythm for more than 95% of the recording time.

The average AHI was 26.4 ± 27.9/h (median: 15/h) in set A and 24.6 ± 21.4/h (median: 20/h) in set B. Patients in set A had a mean age of 54.7 ± 11.4 years vs. 67.9 ± 4.0 years in set B.

### *ECG preprocessing*

Mains interference, in the ECG was suppressed by means of a 50 Hz notch-filter. Subsequently, QRS complexes were detected and semi-automatically classified.

### *QRS area calculation*

We assessed modulation of the QRS amplitude by beat-to-beat estimation of the absolute area under the QRS complex. To this end, we summed the magnitudes of the baseline-corrected ECG in a 120 ms window centered at the QRS triggers [8]. In the remainder of the text, this is referred to as the Q*-series.

### *RMI extraction*

The RMI often can visually be identified as a noise superposition on top of the ECG [Fig. 1(a)—trace 1]. A straightforward way to its extraction is cancellation of the ECG. We have recently suggested a cancellation method in the context of non-invasive fetal ECG extraction [9] that also can be used for RMI extraction. It starts from the baseline- and powerline-filtered raw ECG signals. First a template (average cardiac cycle) is formed and continuously subtracted from the ECG [Fig. 1(a)—trace 2]. The residual variability related to the ECG waves is further attenuated by elimination of the largest principal components of vector ensembles, that are derived from separate epochs comprising the QRS-complex ([R-100 ms; R + 100 ms]), P-wave ([R-300 ms; R-100 ms]) and T-wave ([R + 100 ms; R + 500 ms]). Trace 3 in Fig. 1(a) shows the raw RMI as result of this process.

In order to quantify the strength of RMI, a time-variant measure of variability needs to be applied to this signal. The raw RMI signal envelope represents an instantaneous index of RMI strength with the time resolution of the ECG. For reasons that will become clear later, we preferred to calculate the raw RMI signal standard deviation (SD) in a sliding windows of 100 ms width. The result is shown in trace 4 of Fig. 1(a) which mirrors the respiratory effort during the 10 s epoch. Please note the central apnea during the interval [5 s; 10 s].

The limits of the sketched approach via template-based ECG cancellation are fairly clear: in case of ventricular arrhythmias, a single average template will not suffice. In case of SVAs and atrio-ventricular conduction disorders, the P-waves will not appear time-locked to the QRS complex and hence their elimination will fail. Both problems can be circumvented by loosening the requirement to fully capture all components of RMI. Instead, only those components, for which no spectral overlap between RMI and the ECG exists, are quantified. By means of high-pass filtering, a significant fraction of the ECG activity, particularly the T- and P-wave, can be suppressed. Fig. 1(a)—trace 5 shows the result of a high-pass filter with 60 Hz cutoff frequency (4th order Butterworth, bi-directional) applied to the ECG in trace 1. What remains from the ECG is mainly QRS-activity superimposed to the high-frequency RMA. Since the QRSs occur only transiently in well-localized parts of the signal, they can be easily avoided by defining exclusion zones (R ±50 ms) which are spared in the sliding-window calculation of the SD. This results in an RMI activity estimate with short interruptions (200 ms) around the QRSs [Fig. 1(a)—trace 6]. Despite the 60 Hz cutoff, the overall time-course closely resembles the "full" RMI activity [Fig. 1(a)—trace 4]. The gaps may be interpolated using e.g. linear or cubic spline interpolation.

By choosing a lower frequency cut-off, a larger fraction of RMI activity may be retained. However, dependent on the ECG morphology, even 60 Hz may be too low to fully suppress P-wave activity. The arrow in trace 6 of Fig. 1(a) at $t = 8$ s identifies a small peak that actually is related to an incompletely eliminated P-wave. So in general, a lower cutoff frequency (e.g. 30 Hz) appears appropriate only for the T-wave. This suggests a third variant for RMI quantification: extract RMI activity as a beat-to-beat series by calculating the SD of the high-pass filtered ECG in a temporal window that covers the T-wave. In our implementation, we chose [R + 80 ms; R + 430 ms]. The position of this window is shown in Fig. 1(a)—trace 5 for the first QRS complex. The resulting RMI-activity is given as a non-equidistantly spaced series of dots in trace 7 of Fig. 1(a). Moreover, the linear and cubic spline interpolation is shown.

### *Respiratory surrogate signals*

For the sake of comparability to our previous work [7], and because of the intended application to a sample with arrhythmias, we extracted the RMI as a beat-to-beat series (M*-series) from the T-wave region with a frequency cutoff of 60 Hz. In both data sets A and B, Q* and M* values related to *ventricular* ectopics were excluded and interpolated. Only in set A, this also holds for supraventricular extra-systoles. Finally, both beat-to-beat series Q* and M* were equidistantly resampled at 3 Hz after cubic spline interpolation resulting in the Q- and M-series.

### *Classification feature*

Our first step in assessment of SRBDs is to detect either presence or absence of disordered breathing in 1-min epochs. We make use of the fact that, owing to the underlying pathomechanism, clinically relevant respiratory events typically occur in a repetitive fashion that elicits characteristic low-frequency modulations in the Q-series and M-series [Fig. 1(b)]. It is the occurrence of those low-frequency modulations (not the actual respiratory modulation!) that we quantify for each 1-min epoch based on cross-correlation. We have termed the corresponding feature local similarity index (LSI) [8], and it is separately applied to the Q- and M-series. A subsequent enhancement increased robustness significantly by requiring the joint occurrence in both of the series as well as in the envelope of the M-series (eM) [7]. We refer to this as the joint local similarity index (jLSI).

### *Classifier and performance assessment*

We performed a receiver-operating characteristics (ROC) analysis of the minute-by-minute LSI and jLSI values. The threshold values corresponding to the point on the ROC-curve geometrically closest to the point of perfect separation were selected as thresholds for classification. This does not provide the best achievable overall accuracy but results in good balance between sensitivity and specificity. Classification performance was assessed using sensitivity, specificity and area under the ROC curve.

### *AHI estimation*

To map the epoch-based result into an apnea–hypopnea index (AHI) which can be used for patient screening, we estimate the number of respiratory events from the dominant low-frequency periodicity in the Q-series. This is performed for each epoch that has been identified as positive with respect to disordered breathing. Accumulation over the entire recording, and normalization of the total event count with respect to recording duration yields the AHI estimate [10].

## Results

Fig. 1(b) shows respiratory signals in the course of three mixed apnea events. Traces 1 and 2 reflect respiratory flow and abdominal effort as assessed in the PSG. The phases of central apnea are characterized by absence of any respiratory modulation. During the obstructive phases, respiratory efforts are present but do not produce ventilation. Traces 3 and 4 show the raw RMI obtained by ECG cancellation and the associated RMI activity quantified as SD in a sliding 100 ms window. Traces 5 and 6 depict the approach of high-pass filtering the ECG (60 Hz) and sparing the QRS (trace 5), or using only the T-wave window (trace 6). All approaches clearly reflect respiration and permit to identify the central apneas, although we find some spurious "background" noise in trace 5 which goes back to incompletely suppressed P-waves. Also, the increasing effort in the obstructive phases, and the strong activity during post-apnea hyperventilation, are evident. The Q-series is shown in trace 7. Here, the contrast between central apnea and respiration is more pronounced. The transition from obstruction to hyperventilation is accompanied by a shift of the signal mean eliciting a low-frequency modulation which is the target of our LSI-feature.

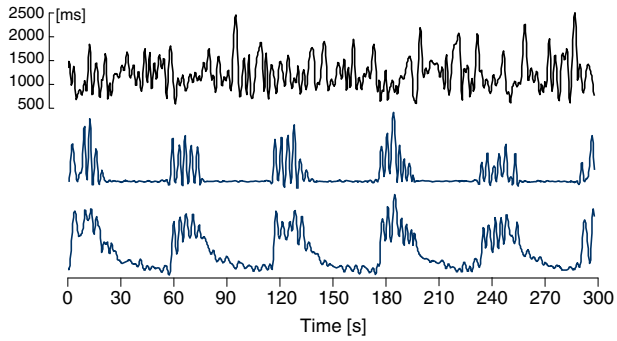


Fig. 2. RR-interval series (upper), M-series (mid) and Q-series (lower) during disordered breathing for a subject with SVA.

Fig. 2 shows exemplary time courses of ECG-derived respiratory signals during ongoing SVA. Despite the highly irregular RR-series, the M-series and the Q-series clearly reflect the respiratory activity and permit to identify disordered breathing.

Table 1 gives the results for minute-by minute SRBD detection in both data sets. Within each group, the LSI-results are similar for both data sources Q and M, and range around 80% sensitivity/83% specificity in set A and 77% sensitivity/72% specificity in set B. This translates to an average reduction of about 3% in sensitivity and 11% in specificity for the arrhythmia set. Despite significant improvement for both sets by data source combination using the jLSI, the between-group difference pertains, resulting in an arrhythmia-set sensitivity of 83.1% and a specificity of 75.0%.

In Fig. 3(a) the corresponding ROC-curves are given. Fig. 3(b) shows the result of the AHI estimation for set B in a scatter-plot with a tendency for overestimation.

## Discussion

This paper presents methods for extraction of the RMI from the ECG and its application to recognition of SRBDs and estimation of the AHI in patients with SVAs. With respect to RMI extraction, our results indicate that the coarser sampling of RMI with 1/beat over the T-wave region is sufficient for detection of SRBDs. As can be seen from the comparison of traces 4–6 in Fig. 1(b), the higher resolution of the sliding-window approaches (traces 4–5) does not significantly add value in this context since all relevant characteristics of respiration are maintained in trace 6. This may, however, be different if exact delineation of the onset/offset of inspiration is required. In settings without SVA, a lower frequency cutoff than 60 Hz may help to improve the signal-to-noise ratio but will definitely require a filter that effectively suppresses power line interference.

Table 1
Classification results for set A and set B.

| Feature | Data source | Data set | Sens. | Spec. | AUC |
|---|---|---|---|---|---|
| LSI | Q | A | 80.9 | 84.0 | 0.892 |
| | | B | 77.5 | 70.4 | 0.807 |
| | M | A | 79.9 | 82.6 | 0.884 |
| | | B | 76.3 | 73.8 | 0.821 |
| jLSI | Q + M + eM | A | 85.5 | 86.0 | 0.919 |
| | | B | 83.1 | 75.0 | 0.843 |

Data source Q refers to the area under the QRS complex, data source M to the respiratory myogram interference (RMI). eM corresponds to the envelope of RMI. Sens: sensitivity, Spec: specificity, AUC: area under the ROC curve.

Focusing on the average classification rate, a considerable reduction of about 3% sensitivity and 11% specificity for the arrhythmia set has to be stated for both the Q series and the M series. At first sight, this suggests that the presence of SVAs does still influence the putatively SV-rhythm-independent base data quantities to at least such an extent that the typical modulations of SRDB become masked or blurred. The strongly varying diastolic filling times in SVAs may be a mechanism that could affect the Q-series e.g. via the Brody effect [11], and the Q-series in Fig. 2 indeed appears a bit more "wiggly" than the M-series, particularly in the phases of central apnea. We observed this also in other cases. But still, our LSI/jLSI approach only targets the low-frequency modulation in the Q-series and consequently should be largely unaffected. For the M-series such a rhythm-influence is even less evident since we would expect the high cutoff frequency (60 Hz) to significantly attenuate potential effects of atrial fibrillation waves onto RMI extraction. A closer look at the ROC curves [Fig. 3(a)] suggests that at least one more aspect should be considered: obviously, the asymmetric reduction in sensitivity and specificity is reflected in the asymmetric way the arrhythmia-set curves deviate from their non-arrhythmic counterparts: the difference in the steep left-hand ascending part is more pronounced than in the flatter right-hand part. The left-hand part corresponds to the increase in sensitivity as the detection threshold is lowered. This increase goes along with a much slower decrease in specificity for the non-arrhythmic data set A. A data check confirmed that the LSI/jLSI values are not generally lower during SVAs. Rather, at least in five cases there exist segments with high LSI/jLSI values that are not annotated as SRBDs and consequently result in false positive detections as also reflected in the tendency for AHI overestimation [Fig. 3(b)]. Manual review of these segments confirmed ongoing apneas with clear desaturations in most cases. The reason why they were not counted as such was that the sleep stage "wake" had to be allocated according to the 30 s epoch based scoring rules. By definition, such formal "wake"-events are not considered as "*sleep* apnea" and do not enter the AHI. Discussing the appropriateness of this practice would go beyond the scope of this paper. However, at least the problems that arise from applying a discrete scoring scale onto a continuous phenomenon are evident. A higher number of wake-stage respiratory events for set B is also documented in the PSG results (46 per record for set B vs. 21 per record for set A). This raises the question whether even SVAs per se might systematically contribute to lighter sleep or increased disquietness during sleep with potential consequences e.g. on overall ECG signal quality.

Clearly, this study suffers from the small sample size of set B which does not permit to give a definite answer and

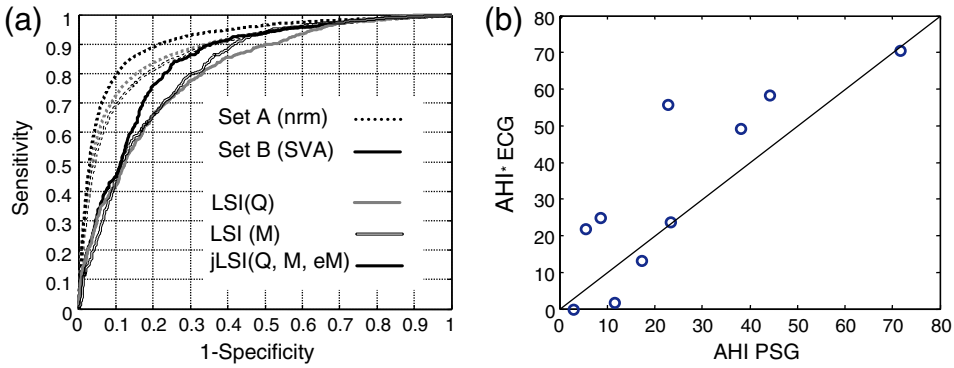


Fig. 3. (a) ROC-curves for the minute-by-minute detection of disordered breathing. Dotted lines correspond to data set A (subjects without SVA), solid lines to data set B (subjects with SVA). The different features are indicated as LSI(M)—double line black, LSI(Q)—single line grey, jLSI(Q, M, eM)—single line black. (b) Scatter diagram of AHI as measured in the PSG vs. AHI as estimated from the ECG for data set B (subjects with SVA).

distinguish potential random findings in our sample from typical SVA-related effects. In conclusion, we observed reduced detection accuracy for SRDBs, in particular reduced specificity in the SVAs group. Still, the study shows that identification of SRBDs from the ECG in the face of SVAs can be expected to be feasible at least for severe cases [Fig. 3(b)] by assessment of modulations in QRS area and RMI. Just as in the arrhythmia-free case, combination of the base-data types Q and M using the jLSI considerably increases detection robustness.

## Acknowledgments

This research was sponsored by a grant of the Internal Junior Research Support Program of Heidelberg University Hospital.

## References

[1] Wang RC, Calvert TW. A model to estimate respiration from vectorcardiogram measurements. Ann Biomed Eng 1974;2(1):47–57.
[2] Somers VK, White DP, Amin R, Abraham WT, Costa F, Culebras A, et al. Sleep apnea and cardiovascular disease: an American Heart Association/American College of Cardiology Foundation Scientific Statement from the American Heart Association Council for High Blood Pressure Research Professional Education Committee, Council on Clinical Cardiology, Stroke Council, and Council on Cardiovascular Nursing. J Am Coll Cardiol 2008;52(8):686–717.
[3] Penzel T, McNames J, Murray A, de Chazal P, Moody G, Raymond B. Systematic comparison of different algorithms for apnoea detection based on electrocardiogram recordings. Med Biol Eng Comput 2002;40(4):402–7.
[4] Guilleminault C, Connolly S, Winkle R, Melvin K, Tilkian A. Cyclical variation of the heart rate in sleep apnoea syndrome. Mechanisms and usefulness of 24 h electrocardiography as a screening technique. Lancet 1984;1(8369):126–31.
[5] Moody GB, Mark RG, Zoccola A, Mantero S. Derivation of respiratory signals from multi-lead ECGs. In: Murray A, editor. Computers in Cardiology, vol. 12. Washington, DC: IEEE Computer Society Press; 1985. p. 113–6.
[6] Einthoven W, Fahr G, de Waart A. Über die Richtung und die manifeste Grösse der Potentialschwankungen im menschlichen Herzen und über den Einfluss der Herzlage auf die Form des Elektrokardiogramms. Pflugers Arch 1913;150:275–315.
[7] Maier C, Wenz H, Dickhaus H. Robust detection of sleep apnea from Holter ECGs. Joint assessment of modulations in QRS amplitude and respiratory myogram interference. Methods Inf Med 2014;53(4):303–7.
[8] Maier C, Wenz H, Dickhaus H. Steps toward subject-specific classification in ECG-based detection of sleep apnea. Physiol Meas 2011;32(11):1807–19.
[9] Maier C, Dickhaus H. Fetal QRS detection and RR interval measurement in noninvasively registered abdominal ECGs. Computing in Cardiology Conference (CinC); 2013. p. 165–8.
[10] Maier C, Wenz H, Dickhaus H. Estimation of the apnea–hypopnea index from epoch-based classification of the ECG using modulations of QRS area and respiratory myogram interference. Computing in Cardiology (CinC); 2012. p. 109–12.
[11] Brody DA. A theoretical analysis of intracavitary blood mass influence on the heart–lead relationship. Circ Res 1956;4:731–8.